Inorg. Chem. **2007**, *46*, 8690–8697

Structure and Properties of Gd_3Ge_4: The Orthorhombic RE_3Ge_4 Structures Revisited (RE = Y, Tb–Tm)

Paul H. Tobash, Gary DiFilippo, and Svilen Bobev*

Department of Chemistry and Biochemistry, University of Delaware, Newark, Delaware 19716

Namjung Hur,[§] Joe D. Thompson, and John L. Sarrao

Materials Physics and Applications Division (MPA), Los Alamos National Laboratory, Los Alamos, New Mexico 87545

Received May 9, 2007

The new binary compound Gd_3Ge_4 has been synthesized and its structure has been determined from single-crystal X-ray diffraction. Gd_3Ge_4 crystallizes in the orthorhombic space group *Cmcm* (No. 63) with unit cell parameters $a = 4.0953(11)$ Å, $b = 10.735(3)$ Å, $c = 14.335(4)$ Å, and $Z = 4$. Its structure can be described as corrugated layers of germanium atoms with gadolinium atoms enclosed between them. The bonding arrangement in Gd_3Ge_4 can also be derived from that of the known compound GdGe (CrB type) through cleavage of the $^1_\infty[Ge_2]$ zigzag chains in GdGe and a subsequent insertion of an extra germanium atom between the resulting triangular fragments. Formally, these characteristics represent isotypism with the Er_3Ge_4 type (Pearson's *oC*28). However, re-examination of the crystallography in the whole RE_3Ge_4 series (RE = Y, Tb–Tm) revealed discrepancies and called into question the accuracy of the originally determined structures. This necessitated a new rationalization of the bonding, which is provided in the context of a comparative discussion concerning both the original and revised structure models, along with an analysis of the trends across the series. The temperature dependence of the magnetic susceptibility of Gd_3Ge_4 shows that it is paramagnetic at room temperature and undergoes antiferromagnetic ordering below 29 K. Magnetization, resistivity, and calorimetry data for several other members of the RE_3Ge_4 family are presented as well.

Introduction

Since the discovery of the giant magnetocaloric effect in Gd_5Ge_4,[1] the interest in the magnetic and crystallographic transformations in this and related Gd−Ge compounds has skyrocketed.[2,3] Today, it is well understood that such phase transitions can be controlled via temperature, pressure, and magnetic field.[3] More recently, attention has been given to the related $Gd_5(Si_xGe_{1-x})_4$ phases, which present a precedent for property tuning via substitution of Ge with the isoelectronic, but smaller in size Si.[4] Analogously, the substitution of Ge for the electron-poorer Ga, as exemplified in $Gd_5(Ga_xGe_{1-x})_4$, or the interchange of alkaline-earth (AE) for rare-earth (RE) metal as exemplified in $RE_{5-x}AE_xGe_4$ (RE = La, Ce, Yb; AE = Mg, Ca) have been shown to subtly affect the structure−bonding−property relationships too.[5]

* To whom correspondence should be addressed. Phone: (302) 831-8720. Fax: (302) 831-6335. E-mail: bobev@udel.edu.

§ Present address: Department of Physics, Inha University, Incheon 402−751, Korea.

(1) Pecharsky, V. K.; Gschneidner, K. A., Jr. *Phys. Rev. Lett*. **1997**, *78*, 4494.

(2) Pecharsky, V. K.; Gschneidner, K. A., Jr. *Adv. Mater*. **2001**, *13*, 683.

(3) (a) Choe, W.; Pecharsky, V. K.; Pecharsky, A. O.; Gschneidner, K. A., Jr.; Young, V. G., Jr.; Miller, G. J. *Phys. Rev. Lett*. **2000**, *84*, 4617. (b) Morellon, L.; Algarabel, P. A.; Ibarra, M. R.; Blasco, J.; García-Landa, B. *Phys. Rev. B*. **1998**, *58*, R 14721. (c) Pecharsky, V. K.; Pecharsky, A. O.; Gschneidner, K. A., Jr. *J. Alloys Compd*. **2002**, *344*, 362. (d) Mozharivskyj, Y.; Pecharsky, A. O.; Pecharsky, V. K.; Miller, G. J. *J. Am. Chem. Soc*. **2005**, *127*, 317. (e) Levin, E. M.; Gschneidner, K. A., Jr.; Pecharsky, V. K. *Phys. Rev. B* **2002**, *65*, 214427. (f) Magen, C.; Arnold, Z.; Morellon, L.; Skorokhod, Y.; Algarabel, P. A.; Ibarra, M. R.; Kamarad, J. *Phys. Rev. Lett.* **2003**, *91*, 207202-1.

(4) (a) Choe, W.; Miller, G. J.; Meyers, J.; Chumbley, S.; Pecharsky, A. O. *Chem. Mater*. **2003**, *15*, 1413. (b) Choe, W.; Pecharsky, A. O.; Wörle, M.; Miller, G. J. *Inorg. Chem.* **2003**, *42*, 8223.

(5) (a) Mozharivskyj, Y.; Choe, W.; Pecharsky, A. O.; Miller, G. J. *J. Am. Chem. Soc*. **2003**, *125*, 15183. (b) Tobash, P. H.; Bobev, S. *J. Am. Chem. Soc*. **2006**, *128*, 3532. (c) Wu, L.-M.; Kim, S.-H.; Seo, D.-K. *J. Am. Chem. Soc*. **2005**, *127*, 15682.

10.1021/ic7009034 CCC: $37.00
Published on Web 09/18/2007

Intrigued by the unique properties of Gd_5Ge_4 and motivated by the recent unexpected discovery of several new binary germanides, Sm_3Ge_5 and Gd_3Ge_5 among others,[6] we focused our attention on the binary Gd−Ge system.[7] This work was specifically aimed at the application of the metal-flux technique[8] toward the synthesis of thermodynamically less-stable (meta-stable) phases for compositions between 50 and 75 atomic percent Ge. Despite the effort to date, this section of the Gd−Ge phase diagram is still not well understood, and a number of poorly characterized phases remain.[9] Moreover, recent differential thermal analyses and computations of the Gibbs free energy for various Gd−Ge compositions have hinted at the possible existence of new binaries in this system.[10]

The initial studies, using molten In as a flux, led to the synthesis of Gd_3Ge_5,[6] and the new ternary compound Gd_2InGe_2.[11] The refinement of the experimental conditions using a different flux, in this case Pb, proved successful and led to the discovery of the new Gd_3Ge_4 compound, the structure and properties of which are the focus of this paper. At first, Gd_3Ge_4 was presumed to be a new member of the orthorhombic Er_3Ge_4 structure type (Pearson's symbol *oC*28; comprising five other RE_3Ge_4 phases RE = Y, Tb−Tm);[12] however, several unusual aspects of its structure prompted our attention to the fact that these might have been overlooked in the earlier studies on RE_3Ge_4,[12] possibly leaving the description of the structure and bonding incomplete. Indeed, these speculations turned factual when the structures of all known RE_3Ge_4 compounds (RE = Y, Tb−Tm) were re-examined. Herein, we also report the revised structures of all "3−4" binaries, along with a side-by-side comparison between the originally proposed and revised models. Reported as well are the electrical resistivity and the heat capacity of two representatives, Ho_3Ge_4 and Er_3Ge_4. A short analysis of the bonding and structural trends across the series are also discussed.

Experimental Section

Synthesis. All manipulations were performed inside an argon-filled glove box with controlled oxygen and moisture levels below 1 ppm or under vacuum. The starting materials, pure elements from Alfa or Ames Laboratory (>99.9%), were used as received. Since the following discussions on the structure and bonding are focused on only one representative of the family, Gd_3Ge_4, a brief description of its synthesis is given below. Further details on the synthesis of Gd_3Ge_4, the general experimental procedures, techniques, and temperature profiles used in the syntheses of the remaining isostructural compounds are listed in the Supporting Information.

The new binary phase Gd_3Ge_4 was serendipitously discovered as a product of a reaction of Gd and Ge in lead flux.[8] This experiment was originally designed to produce large crystals of Gd_3Ge_5, the structure and the properties of which were recently reported by us.[6] The lead-flux reaction yielded small crystals in ∼30−40% yield. In subsequent experiments aimed at the synthesis of Gd_3Ge_4 in larger yield, without the use of metal flux, the elements were loaded with the stoichiometric Gd/Ge ratio and arc melted. This experimental procedure proved less successful because the desired Gd_3Ge_4 was never obtained as a pure phase; the polycrystalline product always contained residual GdGe and $GdGe_{2-x}$. Because of these impurities, physical property measurements were not carried out on samples prepared using this method. Instead, flux-grown crystals were hand-picked under a microscope and were used for the measurements (because of the very different appearance of the Gd_3Ge_4 crystals and the side product $GdPb_3$, they were easily distinguished from one another).

Both the crystals and the powder of Gd_3Ge_4 appear air- and moisture-stable over extended periods of time.

Powder X-ray Diffraction. X-ray powder diffraction patterns were taken at room temperature on a Rigaku MiniFlex powder diffractometer using Cu Kα radiation. Typical runs included $\theta-\theta$ scans ($2\theta_{max} = 70°$) with scan steps of 0.05° and 5 s step^{-1} counting time. The data analysis was carried out using the JADE 6.5 software package. The intensities and the positions of the experimentally observed peaks and those calculated from the crystal structures matched very well. Graphical representation of the experimental and simulated powder pattern of Gd_3Ge_4, along with tabulated intensities and *h k l* indices are provided as Supporting Information (Figure S1 and Table S1). Powder diffraction patterns of the annealed samples of Gd_3Ge_4 are also included as Supporting Information (Figure S2).

Single-Crystal X-ray Diffraction and Structure Refinements. A crystal of Gd_3Ge_4 was chosen from a lead flux reaction and cut to suitable dimensions for data collection (∼0.05 mm^3). It was then mounted on a glass fiber using Paratone N oil and placed on the goniometer. A full sphere of single-crystal X-ray diffraction data were collected at 120 K on a Bruker SMART CCD-based diffractometer. Afterward, a full sphere of data was collected at room temperature as well. The data collections were handled routinely in batch runs at different ω and ϕ angles. The frame width was 0.5° in ω and θ with a data acquisition time of 10 s frame^{-1}. The data collection was carried out with SMART;[13a] data integration and unit cell refinement using all data were done with the program SAINT.[13] A semiempirical absorption correction based on equiva-

(6) Tobash, P. H.; Lins, D.; Bobev, S.; Hur, N.; Thompson, J. D.; Sarrao, J. L. *Inorg. Chem.* **2006**, *45*, 7286.
(7) Villars, P.; Calvert, L. D. *Pearson's Handbook of Crystallographic Data for Intermetallic Phases*, 2nd ed.; American Society for Metals: Materials Park, OH, 1991.
(8) (a) Canfield, P. C.; Fisk, Z. *Philos. Mag. B* **1992**, *65*, 1117. (b) Kanatzidis, M. G.; Pöttgen, R.; Jeitschko, W. *Angew. Chem., Int. Ed.* **2005**, *44*, 6996.
(9) Massalski, T. B. *Binary Alloy Phase Diagrams*; American Society for Metals: Materials Park, OH, 1990.
(10) (a) Uspenskaya, I. A.; Goryacheva, V. I.; Kutsenok, I. B. *Russ. J. Phys. Chem.* **2001**, *75*, S135. (b) Polotskaya, R. I. *Poroshk. Metall.* **1991**, *337*, 64. (c) Gorbachuk, N. P.; Bolgar, A. S. *Powder Metall. Met. Ceram.* **1999**, *38*, 462.
(11) Tobash, P. H.; Lins, D.; Bobev, S.; Lima, A.; Hundley, M. F.; Thompson, J. D.; Sarrao, J. L. *Chem. Mater.* **2005**, *17*, 5567.
(12) (a) Oleksyn, O. Ya.; Bodak, O. I. *J. Alloys Compd.* **1994**, *210*, 19. (b) Ijjaali, I.; Venturini, G.; Malaman, B. *J. Alloys Compd.* **1999**, *284*, 237. (c) Belyavina, N. M.; Markiv, V. Y.; Speka, M. V. *J. Alloys Compd.* **1999**, *283*, 162. (d) Zaharko, O.; Schobinger-Papamantellos, P.; Ritter, C.; Janssen, Y.; Brück, E.; de Boer, F. R.; Buschow, K. H. J. *J. Phys.: Condens. Matter* **1998**, *10*, 2881. (e) Zaharko, O.; Schobinger-Papamantellos, P.; Sikora, W.; Ritter, C.; Janssen, Y.; Brück, E.; de Boer, F. R.; Buschow, K. H. J. *J. Phys.: Condens. Matter* **1998**, *10*, 6553. (f) Oleksyn, O.; Schobinger-Papamantellos, P.; Ritter, C.; Janssen, Y.; Brück, E.; Buschow, K. H. J. *J. Phys.: Condens. Matter* **1997**, *9*, 9993. (g) Oleksyn, O.; Schobinger-Papamantellos, P.; Ritter, C.; de Groot, C. H.; Buschow, K. H. J. *J. Alloys Compd.* **1997**, *262*, 492. (h) Schobinger-Papamantellos, P.; Oleksyn, O.; Ritter, C.; de Groot, C. H.; Buschow, K. H. J. *J. Magn. Magn. Mater.* **1997**, *169*, 253. (i) Janssen, Y.; Brück, E.; de Groot, C. H.; Kayzel, F. E.; de Boer, F. R.; Buschow, K. H. J.; Oleksyn, O.; Schobinger-Papamantellos, P. *J. Magn. Magn. Mater.* **1998**, *177*, 1147.
(13) (a) *SMART NT*, version 5.63; Bruker Analytical X-ray Systems, Inc.: Madison, WI, 2003. (b) *SAINT NT*, version 6.45; Bruker Analytical X-ray Systems, Inc.: Madison, WI, 2003.

Table 1. Selected Crystal Data and Structure Refinement Parameters for Gd_3Ge_4

empirical formula	Gd_3Ge_4
fw	762.11 g/mol
data collection temp	120(2) K
radiation	Mo Kα
wavelength (λ)	0.71073 Å
cryst syst	orthorhombic
space group	*Cmcm* (No. 63)
unit cell dimensions[a]	$a = 4.0953(11)$ Å
	$b = 10.735(3)$ Å
	$c = 14.335(4)$ Å
unit cell volume	630.2(3) Å^3
Z	4
density (ρ_{calcd})	8.032 g/cm^3
abs coeff (μ)	49.772 mm^{-1}
final R indices[b]	R1 = 0.0217
[$I > 2\sigma_{(I)}$]	wR2 = 0.0492
final R indices[b]	R1 = 0.0238
[all data]	wR2 = 0.0501

[a] Cell parameters at 293(2) K: $a = 4.1017(16)$ Å, $b = 10.750(4)$ Å, $c = 14.348(6)$ Å. [b] $R1 = \sum||F_o| - |F_c||/\sum|F_o|$; $wR2 = [\sum[w(F_o^2 - F_c^2)^2]/\sum[w(F_o^2)^2]]^{1/2}$, $w = 1/[\sigma^2F_o^2 + (0.025P)^2 + 6.40P]$, $P = (F_o^2 + 2F_c^2)/3$.

lents was applied using SADABS.[14a] The structure was solved by direct methods and refined by the full matrix least-squares on F^2 method using SHELX.[14b] Further details of the data collection and structure refinements parameters are given in Table 1. Analogous information for the remaining six compounds is summarized in Tables S2 and S3 (Supporting Information).

At the early stages of the structure elucidation, the originally proposed structure (Er_3Ge_4 type,[12a] Pearson's symbol *oC*28) was assumed to be correct and was adopted for the refinements. The initial cycles with isotropic thermal parameters confirmed the overall suitability of the model and converged to reasonable residuals (R1 and wR2 were about 5 and 10%, respectively). In the next set of refinements, when all atoms were refined with anisotropic displacement parameters (ADP), a problem with the ADP for one of the Ge atoms (referred to as Ge1 hereafter[15]) became apparent: from the segment of the structure depicted in Figure S3, the abnormal elongation of the ADP of Ge1 ($U_{33} > U_{22} \gg U_{11}$) can be clearly seen. Analyses of the Fourier and corresponding difference Fourier maps indicated that the electron density at this site was not localized and could be the artifact of an averaged density from two statistically distributed germaniums (for representative plots clearly showing the two maxima, see Supporting Information Figure S3). This, coupled with the fact that the site occupancy did not deviate significantly from full when freed to refine, suggested the presence of a previously overlooked positional or dynamic disorder. Similar problems have also been reported for the isoelectronic, but not isostructural, RE_3Si_4 (RE = Dy, Ho) compounds.[16] Indeed, an almost identical anomaly of the anisotropic displacement parameter of one of the silicon sites (Si3) in these structures is explained by "a deviation from the mirror plane" and a possible Si underoccupancy.[16b]

Table 2. Atomic Coordinates and Equivalent Isotropic Displacement Parameters (U_{eq}[a]) for Gd_3Ge_4[b]

atom	Wyckoff position	x	y	z	U_{eq} (Å^2)
Gd1	8*f*	0	0.3313(1)	0.0967(1)	0.0088(2)
Gd2	4*c*	0	0.0442(1)	1/4	0.0086(2)
Ge1[c]	8*f*	0	0.0237(2)	0.0194(2)	0.0123(6)
Ge2	8*f*	0	0.6202(1)	0.1093(1)	0.0106(3)
Ge3	4*c*	0	0.7708(2)	1/4	0.0102(3)

[a] U_{eq} is defined as one-third of the trace of the orthogonalized U_{ij} tensor. [b] The atomic coordinates for RE_3Ge_4 (RE = Y, Tb−Tm) are very similar and are given as Supporting Information. [c] 50% occupied. The original structure determination[12] has Ge1 at 4*a* (0, 0, 0). If Ge1 is refined at this position, its anisotropic displacement parameter is abnormally elongated: $U_{11} = 0.010(1)$, $U_{22} = 0.068(2)$, $U_{33} = 0.086(3)$, $U_{23} = 0.065(2)$, $U_{13} = 0$, $U_{12} = 0$.

In the present case, the side-by-side comparison of the low-temperature and room-temperature diffraction data did not indicate a significant difference between the shape and the size of the ADP of the problematic Ge1. Additionally, the search for weak reflections (through long-exposure zone images at both temperatures), which violate the global symmetry or which can be indexed based on a larger unit cell, did not verify the hypotheses that either a lower symmetry structure or an ordered superstructure exist. We also bring attention to the previous neutron diffraction work on RE_3Ge_4 (RE = Tb−Tm),[12] which provides additional evidence in support of this and proves that there are no structural transitions as a function of the temperature down to 1.7 K.

On the basis of the above, the Ge1 disorder was believed to be purely statistical (not dynamic) and best modeled by removing the local 2-fold symmetry. After a careful inspection of the electron density (Figure S3), this symmetry reduction was done by displacement of Ge1 ~0.3 Å away from its originally proposed position in direction approximately parallel to [011]. In the new model, the new coordinates for Ge1 are 0, *y*, *z* (Wyckoff 8*f*, Table 2). The Hamilton *R*-value test[17] was performed to determine whether the new model led to *significant* improvement in the agreement between the observed and the calculated structure factors. The test proved unequivocally, at a significance level of 0.005, that the improvement in the global refinement is not simply an artifact of the addition of extra refinement parameters. However, the drawback of such reduction of the point symmetry (from 2/*m* to *m*) was that it necessitated refining the "new" site as partially occupied. The occupancy refined close to a half, and it was later set to 1/2 (fixed). This was justified because there was no experimental evidence to suggest any possible phase width. The remaining four atomic positions were well-behaved and were not significantly affected by the "split" of Ge1. We also note that model refinements in subgroups of *Cmcm* were attempted but did not resolve the problem with the Ge1 either.

In the last refinement cycles, the five atomic positions for Gd_3Ge_4 were standardized using STRUCTURE TIDY.[15] Final positional and equivalent isotropic displacement parameters are listed in Table 2; important bond distances and angles are listed in Table 3. The crystallographic information file (CIF) has also been deposited with Fachinformationszentrum Karlsruhe, 76344 Eggenstein-Leopoldshafen, Germany, (fax: (49) 7247−808-666; e-mail: crysdata@fiz.karlsruhe.de), depository number CSD-418018.[18]

Magnetic Susceptibility Measurements. Field-cooled dc magnetization (M) measurements were performed for a ~10 mg sample of Gd_3Ge_4 using a Quantum Design $MPMS_2$ SQUID magnetometer. The measurements were taken in the temperature range from 5 to

(14) (a) *SADABS NT*, version 2.10; Bruker Analytical X-ray Systems, Inc.: Madison, WI, 2001. (b) *SHELXTL*, version 6.12; Bruker Analytical X-ray Systems, Inc.: Madison, WI, 2001.

(15) This atom occupies the site with symbol Wyckoff 4*a* (coordinates 0, 0, 0) and is labeled herein as Ge1. We point out that the use of STRUCTURE TIDY (Gelato, L. M.; Parthe, E. *J. Appl. Crystallogr.* **1987**, *20*, 139) to standardize the coordinates interchanges the labels of Ge1 and Ge3 from the older literature.

(16) (a) Roger, J.; Guizouarn, T.; Hiebl, K.; Halet, J.-F.; Guérin, R. *J. Alloys Compd.* **2005**, *394*, 28. (b) Ijjaali, I.; Venturini, G.; Malaman, B. *J. Alloys Compd.* **1998**, *269*, L6. (c) Roger, J.; Babizhetskyy, V.; Hiebl, K.; Halet, J.-F.; Guérin, R. *J. Alloys Compd.* **2006**, *407*, 25.

(17) Hamilton, W. C. *Acta Crystallogr.* **1965**, *18*, 502.

Table 3. Selected Bond Distances (Å) and Angles (deg) in Gd_3Ge_4

revised model			original model		
Ge1	Ge2 (×2)	2.632(2)	Ge1	Ge2 (×4)	2.833(2)
Ge2	Ge3	2.585(2)	Ge2	Ge3	2.588(4)
	Ge1 (×2)	2.632(2)		Ge1 (×2)	2.833(2)
Ge3	Ge2 (×3)	2.585(2)	Ge3	Ge2 (×3)	2.588(4)
Gd1	Ge1 (×2)	3.064(2) (or 3.112(2))	Gd1	Ge1 (×2)	3.065(1)
	Ge2	2.999(1)		Ge2	2.997(3)
	Ge2 (×2)	3.060(1)		Ge2 (×2)	3.059(2)
	Ge2	3.107(2)		Ge2	3.107(2)
	Ge3 (×2)	3.073(1)		Ge3 (×2)	3.072(1)
Gd2	Ge1 (×2)	3.313(2)	Gd2	Ge1 (×2)	3.615(2)
	Ge2 (×4)	2.988(1)		Ge2 (×4)	2.989(2)
	Ge3	2.935(2)		Ge3	2.932(4)
	Ge3 (×2)	3.178(2)		Ge3 (×2)	3.182(3)
Ge1−Ge2−Ge1		102.14(8)	Ge1−Ge2−Ge1		90.53(8)
Ge1−Ge2−Ge3		128.93(4)	Ge1−Ge2−Ge3		134.73(4)
Ge2−Ge3−Ge2		102.56(8)	Ge2−Ge3−Ge2		102.6(2)

290 K and in an applied magnetic field (H) of 500 Oe. The raw magnetization data were corrected for the holder contribution and converted to molar susceptibility ($\chi_m = M/H$, normalized per mole of Gd). The measured sample consisted of carefully selected crystals, and the phase purity was subsequently assessed by powder X-ray diffraction.

Specific Heat and Resistivity Measurements. The electrical resistivity and the heat capacity were measured in a commercial Quantum Design PPMS system. The resistance was measured using the four-probe technique from 2 to 300 K with an excitation current of 1 mA. The contacts to the surface of the chosen single crystals of Ho_3Ge_4 and Er_3Ge_4 (grown by In flux, both longer than 3 mm) were made by spot welding. Calorimetry data for the same specimens were taken using the thermal relaxation method. Measurements for Gd_3Ge_4 are not reported because the crystals were too small to ensure reproducible results.

Results and Discussion

Synthesis, Structure, and Bonding. Gd_3Ge_4 crystallizes in the centrosymmetric space group *Cmcm* (No. 63), and its structure contains five crystallographically unique atoms in the asymmetric unit, all in special positions (Table 2). Formally, the structure can be classified with the orthorhombic Er_3Ge_4 type or its ordered ternary derivative W_3CoB_3 (Pearson's code *oC*28);[7] however, as shown below, there are subtle differences between the originally proposed[12] and herein discussed models. To prove that the new description is better suited to explain the crystal chemistry in this class of intermetallic compounds, the structures of the six known germanides that crystallize with the Er_3Ge_4 type have also been revised.

At a first glance, the Gd_3Ge_4 structure can be readily described as wavelike "layers" of germanium atoms with gadolinium atoms enclosed between them, as shown in Figure 1. The layers propagate parallel to the *ac*-plane and are assembled in space by packing along the *b*-crystallographic direction. A more detailed description of the structure can be given once its close relationship with another ubiquitous structure is recognized, namely, that of GdGe with the CrB type.[7] Following this line of thought, the structure of Gd_3Ge_4 can be very conveniently derived from that of GdGe (space group *Cmcm*, $a \approx 4.3$ Å, $b \approx 10.8$ Å, $c \approx 4.0$ Å)[19] through breaking of the Ge-chains into triangular fragments and the insertion of an additional germanium atom between them. This imaginary "process" accounts for not only the structure but also the composition of the title compound according to the balanced equation

$$3 \times \mathrm{GdGe} + \mathrm{Ge} = \mathrm{Gd_3Ge_4}$$

With the cut-and-paste approach schematically illustrated in Figure 2, it is evident that the formal opening of every third Ge−Ge bond from the infinite Ge-chains in GdGe, coupled with a small distortion around the broken bonds, will result in two-dimensional slabs with exactly the same topology as those in Gd_3Ge_4. These slabs are made of "isolated" Ge-trimers (drawn in blue), which are stacked on top of each other in the direction of the *b*-axis (Figure 2; note that in the chosen projections, the unit cell axes for both GdGe and Gd_3Ge_4 are collinear). The GdGe slabs and the layers of extra Ge run parallel to the *ab*-plane and form a hexagonal-like (i.e., AA′BB′AA′BB′) array along the direction of the *c*-axis (Figure 2).

An alternative description can be given in terms of slightly distorted trigonal prisms of gadolinium atoms (drawn in red), centered by germanium atoms, Ge3 in the current notation. Such Gd_6-prisms share common triangular faces along the direction of the *a*-axis (the viewing direction in Figure 2) and are arranged in an eclipsed fashion in a perpendicular direction, that is, along the *b*-axis. Two of the prisms' rectangular faces are capped by Ge atoms (Ge2), and the third face is capped by a Gd atom from an adjacent prism. The addition of an extra Ge atom, Ge1 in the current notation, between the GdGe slabs, will "bridge" them through four

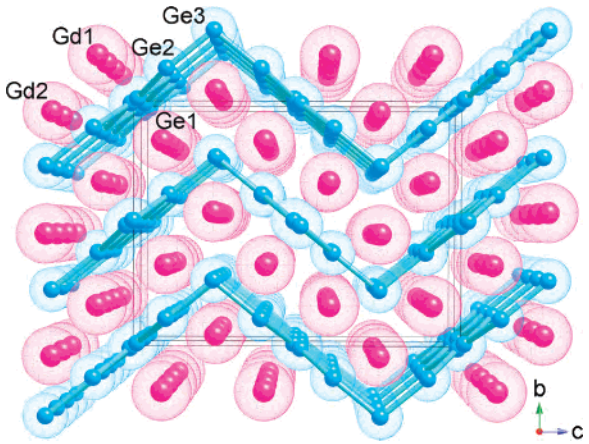

Figure 1. Perspective view of the orthorhombic structure of Gd_3Ge_4, viewed down the *a*-axis. Ball-and-stick and space filling representations are superimposed to emphasize the way atoms are packed. Gd atoms are shown as red spheres, and the Ge atoms are drawn as light-blue spheres. The unit cell is outlined.

(18) The revised atomic coordinates and bond distances for the isostructural RE_3Ge_4 compounds (RE = Y, Tb−Tm) are provided as Supporting Information. The crystallographic information files (CIF) have also been deposited with Fachinformationszentrum Karlsruhe [76344 Eggenstein-Leopoldshafen, Germany; fax: (49) 7247−808-666; email: crysdata@fiz.karlsruhe.de; depository numbers CSD-418019 (Tb_3Ge_4), CSD-418020 (Dy_3Ge_4), CSD-418021 (Ho_3Ge_4), CSD-418022 (Er_3Ge_4), CSD-418023 (Tm_3Ge_4), and CSD-418028 (Y_3Ge_4).

(19) Hohnke, D.; Parthé, E. *Acta Crystallogr.* **1966**, *20*, 572.

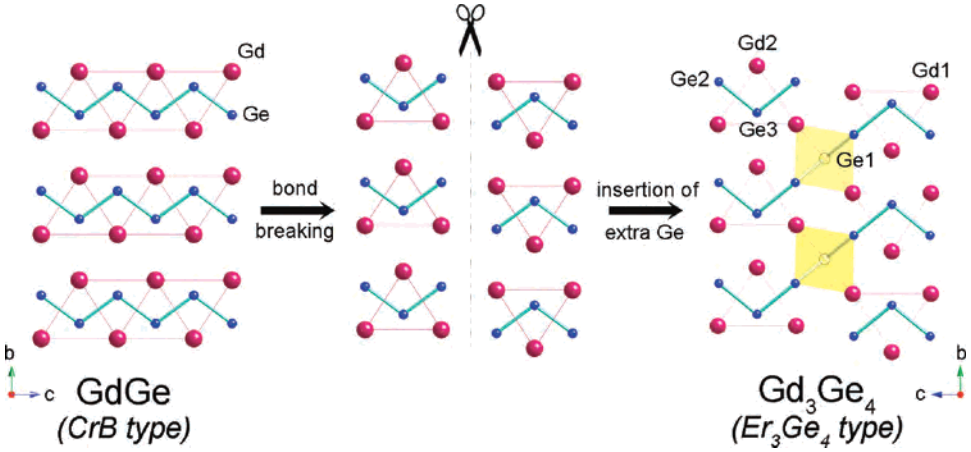

Figure 2. A schematic representation of the process of breaking every third Ge−Ge bond from the polyene-like chains in GdGe and inserting an extra Ge in the "empty space" to form the structure of Gd_3Ge_4. Color code as in Figure 1. The extra Ge atoms (Ge1 in the current notation) are shown at the centers of yellow translucent polyhedra of four germanium and four gadolinium atoms.

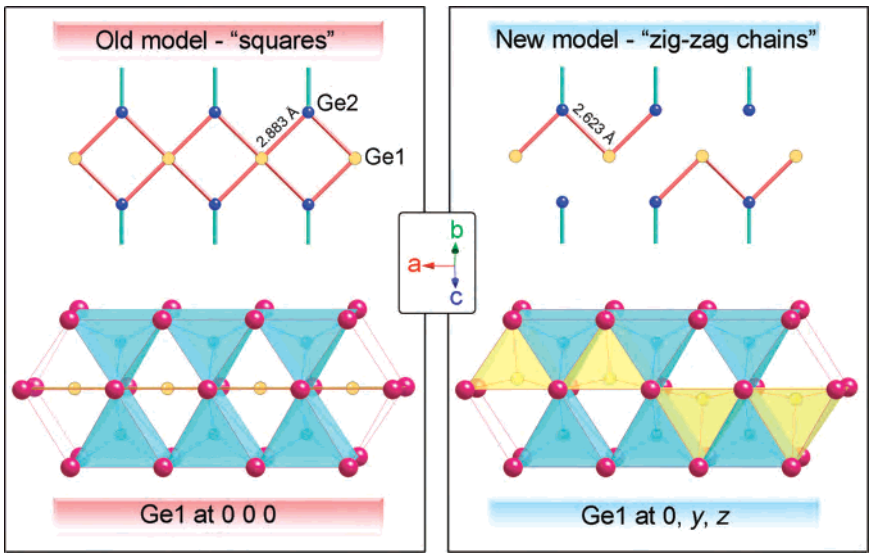

Figure 3. Schematic representation of the Ge1 bonding and coordination. The originally proposed and the revised structural models are compared: see text for details.

opposing germanium and a nearly orthogonal set of four gadolinium atoms from neighboring units (Figure 2, drawn in yellow). Such coordination of a germanium atom is rather unusual and is the most likely reason for the observed positional disorder (Figure 3). Realization of this occurrence results in important differences in the structure and bonding description, and these are discussed in detail in the following paragraphs.

In the originally proposed model for the "3−4" structure,[12] Ge1 is located at the origin (0, 0, 0; Wyckoff 4*a*). This means that the germanium atoms at Ge1 and the next-nearest neighbors (Ge2) form squares (or rather rhombi) with an unusually long Ge−Ge distance of 2.833(2) Å (Table 3). The corresponding Ge2−Ge1−Ge2 angle is 90.53(4)°, indicating that Ge1 is nearly square-planar (Figure 3). Such an environment is not common for molecular species of the group 14 elements,[20] but it is not without a precedent among the extended structures of intermetallic compounds. Indeed, there are a number of binary phases, some not devoid of disorder, whose structures feature polyanionic networks based on square-planar Ge or Sn: $TmGe_{1.9}$,[21a] Er_2Ge_5,[21b] $NaSn_5$,[21c] $LaGe_5$,[21d] $SnSn_4$,[21e] among others. Long Ge−Ge contacts and angles in the same range are also known between the *basal* Ge atoms in the structures of RE*T*Ge_2 ($CeNiSi_2$ type, T = late transition metal) for instance;[7] however, the germanium interactions in these ternary compounds are very different than the ones in Gd_3Ge_4. The contribution of the transition metal to the bonding is considerable, and such structures are typically described in terms of layers of *T*Ge_4 square pyramids that are fused at their bases in an alternating manner (PbO-type layers).[22]

(20) (a) Hoffmann, R.; Alder, R. W.; Wilcox, C. F. *J. Am. Chem. Soc.* **1970**, *92*, 4992. (b) Pancharatna, P. D.; Méndez-Rojas, M. A.; Merino, G.; Vela, A.; Hoffmann, R. *J. Am. Chem. Soc.* **2004**, *126*, 15309. (c) Yoshizawa, K.; Suzuki, A. *Chem. Phys.* **2001**, *271*, 41. (d) Wang, Z.-X.,; Schleyer, P. V. *J. Am. Chem. Soc.* **2001**, *123*, 994.

(21) (a) Venturini, G. *J. Alloys Compd.* **2000**, *308*, 200. (b) Venturini, G.; Ijjaali, I.; Malaman, B. *J. Alloys Compd.* **1999**, *288*, 183. (c) Fässler, T. F.; Kronseder, C. *Angew. Chem., Int. Ed.* **1998**, *37*, 1571. (d) Fukuoka, H.; Yamanaka, S. *Phys. Rev. B* **2003**, *67*, 094501. (e) Hoffmann, S.; Fässler, T. F.; *Inorg. Chem.* **2003**, *42*, 8748.

(22) (a) Zheng, C.; Hoffmann, R. *J. Am. Chem. Soc.* **1986**, *108*, 3078. (b) Burdett, J. K.; Miller, G. J. *Chem. Mater.* **1990**, *2*, 12. (c) Hlukhyy, V.; Eck, S.; Fässler, T. F. *Inorg. Chem.* **2006**, *45*, 7408. (d) Proserpio, D. M.; Chacon, G.; Zheng, C. *Chem. Mater.* **1998**, *10*, 1286.

In the revised model for the "3−4" structure, little changes in the global structure description aside from the connectivity of the Ge1 atoms. For example, the refined Ge−Ge distance between the other two crystallographically distinct germaniums, Ge2 and Ge3 is now 2.585(2) Å (compared to 2.588(4) Å from the previously discussed refinement), and the corresponding Ge2−Ge3−Ge2 angle is 102.56(8)° (Table 3). Such distances and angles are "normal" and compare well with the ones reported for other binary rare-earth or alkaline-earth germanides, where the germaniums are in partially reduced oxidation states (for GdGe, d_{Ge-Ge} is on the order of 2.6 Å, and the angle is about 100°).[6,19,23−26] However, this is not the case with the long distances and angles around the nearly square-planar Ge1, which adjust significantly upon moving Ge1 away from the origin. This effectively means that the Ge-"squares" from the original model break into zigzag chains which run along the *a*-axis (Figure 3). Unlike the square-planar Ge, the $^1_\infty[Ge_2]$ chains in the revised description and the way they interconnect like fragments in an orthogonal direction are a common structural element in the crystal chemistry of many silicides and germanides.[7,27,28] In particular, such arrangement is reminiscent of the α-$ThSi_2$ structure type (and its derivatives), which can be viewed as formed by sets of mutually perpendicular polyene-like chains.[29,30] We note here that the bonding in various such chains and layers of the heavier carbon analogs has already been thoroughly analyzed;[30] therefore, we focus the remainder of discussion on the specifics of the revised structural model.

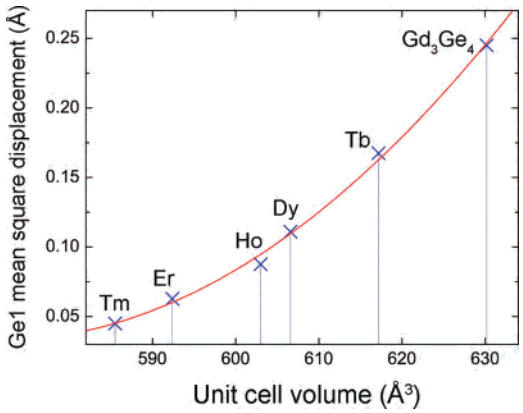

Figure 4. Correlation between the unit cell volumes (Å^3) for RE_3Ge_4 (RE = Gd−Tm) and the longest mean square displacement parameter of the Ge1 atom (refined at 0, 0, 0 from room-temperature data). The deviation is most pronounced for Gd through Dy and becomes progressively smaller near the end of the *f*-block.

An important consequence of this new model, which needs to be specifically emphasized, is the fact that the germanium sub-network is relieved from the "strain" of the square-planar Ge.[28] This is clearly shown by the Ge1−Ge2 distance, now 2.632(2) Å, and the Ge2−Ge1−Ge2 angle, now 102.14(8)° (Figure 3a). Such distances and angles are comparable with the Ge2−Ge3 contacts and the Ge2−Ge3−Ge2 angles, which remain virtually unaffected by the "split" of the Ge1 site (Table 3). Allowing the Ge1 to "relax" has an implication over the gadolinium polyhedra as well (Figure 3b). In the revised structural model, instead at the center of a Gd-square, Ge1 is located inside a trigonal prism of six nearest Gd atoms, with distances in the range from 3.064(2) to 3.313(2) Å (Table 3). This coordination resembles very much the trigonal prismatic environment of the other two sites, Ge2 and Ge3. A survey of the structure types adopted by many other lanthanide-based intermetallics indicates that prisms, not squares are the most recurring motifs.[28] Graphical representations of the Gd coordination polyhedra are shown in Supporting Information (Figure S4).

The in-depth analyses of the bonding interactions in all isostructural compounds show that the Ge-distances and angles are almost invariant of the nature of the rare-earth metal, comparison of all structural parameters for the remaining six compounds is provided in tabular form as Supporting Information (Tables S2 and S3). This does not, however, provide any evidence for a correlation with the variations of the unit cell parameters when moving across the series. The only systematic trend that was noted occurs between the size of the rare-earth metal and the degree of disorder as measured by the longest mean square displacement parameter for Ge1 (for anisotropic displacement parameters, please see the CIF in Supporting Information). This dependence is shown graphically in Figure 4: the unit cell volume of RE_3Ge_4 (RE = Gd−Tm) is plotted as a function of the elongation of the displacement parameter for Ge1 when it is refined at coordinates 0, 0, 0 (original model). From the plot, it is clear that as the unit cell volume decreases, the elongation of the thermal parameter becomes progressively smaller. This is easy to understand because the size of the available "empty space" around Ge1 will be

(23) Because the GdGe structure is not completely refined, a more accurate comparison is not possible; we also note that there are more than three sets of different unit cell constants at room temperature, see ref 19 or Tharp, A. G.; Smith, G. S.; Johnson, Q. *Acta Crystallogr.* **1966**, *20*, 583.

(24) (a) Bobev, S.; Bauer, E. D.; Thompson, J. D.; Sarrao, J. L.; Miller, G. J.; Eck, B.; Dronskowski, R. *J. Solid State Chem.* **2004**, *177*, 3545. (b) Tobash, P. H.; Bobev, S. *J. Solid State Chem.* **2007**, *180*, 1575.

(25) (a) Budnyk, S.; Weitzer, F.; Kubata, C.; Prots, Y.; Akselrud, L. G.; Schnelle, W.; Hiebl, K.; Nesper, R.; Wagner, F. R.; Grin, Y. *J. Solid State Chem.* **2006**, *179*, 2329. (b) Schobinger-Papamantellos, P.; Buschow, K. H. J. *J. Magn. Magn. Mater.* **1989**, *82*, 99. (c) Schobinger-Papamantellos, P.; Buschow, K. H. J. *J. Less-Common Met.* **1989**, *146*, 279. (d) Venturini, G.; Ijjaali, I.; Malaman, B. *J. Alloys Compd.* **1999**, *285*, 194. (e) Venturini, G.; Ijjaali, I.; Malaman, B. *J. Alloys Compd.* **1999**, *284*, 262. (f) Schobinger-Papamantellos, P.; de Mooij, D. B.; Buschow, K. H. J. *J. Less-Common Met.* **1990**, *163*, 319.

(26) Vaughey, J. T.; Miller, G. J.; Gravelle, S.; Leon-Escamilla, E. A.; Corbett, J. D. *J. Solid State Chem.* **1997**, *133*, 501.

(27) Because of the symmetry reduction and the resultant close separation between the symmetry-equivalent Ge1 atoms in this model, Ge1 has to be treated with 50% occupancy (Figure 3). This may be envisioned as either breaking the chains along the crystallographic *a*-axis (a scenario depicted in Figure 3) or by having infinite chains along the *a*-axis that bridge the GdGe slabs on either their left or their right side (refer to Figure 2 for directions). Both schemes, in principle, may result in full or partial order in any direction, but since the experimental data do not corroborate such hypothesis, an entirely statistical distribution is assumed.

(28) Szytula, A., Leciejewicz, J., Eds. *Handbook of Crystal Structures and Magnetic Properties of Rare Earth Intermetallics*; CRC Press: Boca Raton, FL, 1994.

(29) (a) Hoffman, R.; Hughbanks, T.; Kertész, M. *J. Am. Chem. Soc.* **1983**, *105*, 4831. (b) Mao, J.-G.; Goodey, J.; Guloy, A. M. *Inorg. Chem.* **2002**, *41*, 931. (c) Guloy, A. M.; Corbett, J. D. *Inorg. Chem.* **1991**, *30*, 4789.

(30) (a) Papoian, G. A.; Hoffmann, R. *Angew. Chem., Int. Ed.* **2000**, *39*, 2409. (b) Zheng, C.; Hoffmann, R. *Inorg. Chem.* **1989**, *28*, 1074.

strongly dependent on the cations' radii;[31] after all, the "thickness" and the "separation" between the CrB-like slabs in Figure 2 is expected to scale with the lanthanide contraction. In other words, the larger the rare-earth metal cation, the more "room" for Ge1 there will be.

Because of this "size dependence", locating the maxima in the Fourier maps and refining the split Ge1 proved to be trivial for Gd−Ho (Figure 4). For Er_3Ge_4 and Tm_3Ge_4 in particular, the two symmetry-equivalent Ge1 atoms are very close (∼0.16−0.20 Å) and are therefore difficult to treat in a model refinement. The Ge1 offset from the origin was determined first when the atom was refined with isotropic thermal parameters and then fixed for the final anisotropic refinement. This difficulty, together with the fact that almost all previous structure determinations have been done from powder crystallography may explain why these aspects of the structure and the bonding have been overlooked in the earlier studies.[12,32]

One can therefore draw a parallel between the "3−4" structures and the structures of the cage compounds, skutterudites and clathrates in particular, where the interstitial atoms occupying the oversized cavities can vibrate or "rattle" about their equilibrium positions. This has been suggested to be an important prerequisite for scattering of the heat-carrying phonons and thereby for lowering the phonon-contributed lattice thermal conductivity, thus making such materials suitable for thermoelectric applications. However, we reiterate that despite the analogy, atom vibrations (dynamic disorder) are not the case here. Another relevant occurrence that could be mentioned here is in the structure of $Ba_2Cd_3Bi_4$ in which of one of the cadmium atoms has an unusual coordination and an elongated ADP. Temperature-dependent crystallography in this instance finds evidence for correlation between the ADP and a rather large thermal expansion along the *b*-axis.[33]

Properties. Temperature-dependent dc magnetization measurements for Gd_3Ge_4 were performed in the 5−290 K range and the resulting plot of the magnetic susceptibility, $\chi = M/H$, versus temperature, T, is shown in Figure 5. Gd_3Ge_4 exhibits a Curie−Weiss paramagnetic behavior at temperatures above 30−35 K. The cusplike feature in the χ(T) data around 29 K indicates the onset of long-range antiferromagnetic order. Above the Néel temperature, $\chi(T)$ follows the Curie−Weiss law $\chi(T) = C/(T - \theta_p)$, where $C = N_A\mu_{eff}^2/3k_B$ is the Curie constant, and yields an effective moment of $\mu_{eff} = 7.82\ \mu_B$ per Gd^{3+}, in good agreement with the theoretically calculated value of 7.94 μ_B according to the Hund's rules for a [Xe]f^7 configuration.[34] The Weiss temperature, θ_p, is negative (−31 K) as expected for an antiferromagnetically ordered structure. The χ(T) plots for four other compounds are provided in the Supporting Information (Figure S5); the results nicely reproduce previous work on RE_3Ge_4 (RE = Tb−Tm), the magnetic structures of which have been elucidated from powder neutron diffraction.[12d−h] Since the revised structure description concerns mostly the Ge subnetwork and does not affect in a significant way the rare-earth metal interactions, further discussion on the magnetic order in the whole 3−4 series is unnecessary; a brief summary of the corresponding Néel temperatures, effective moments and Weiss constants is given in Table 4.

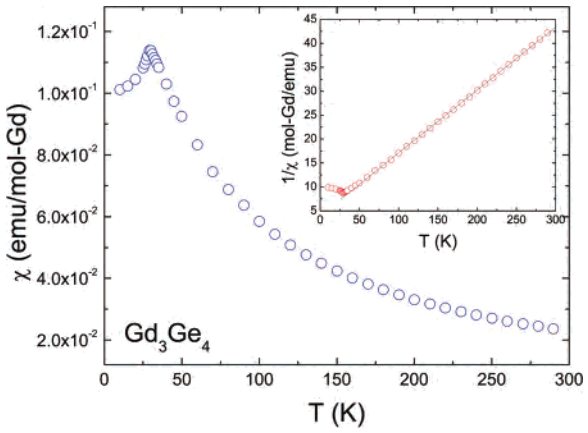

Figure 5. Temperature dependence of the magnetic susceptibility (χ_m) of Gd_3Ge_4, measured in a magnetic field of 500 Oe. Inverse magnetic susceptibility $\chi^{-1}(T)$ plot is shown in the inset.

Table 4. Selected Physical Property Data for RE_3Ge_4 (RE = Y, Gd−Tm)[a]

	magnetic behavior	μ_{eff} (μ_B)[b]	T_N (K)[c]	θ_p (K)	ρ_{298} ($\mu\Omega$ cm)	ref
Y_3Ge_4	**Pauli paramagnetic**					**this work**
Gd_3Ge_4	**antiferromagnetic**	**7.82**	**29**	**−31**		**this work**
Tb_3Ge_4	antiferromagnetic	9.76	28	−22		12f
Dy_3Ge_4	antiferromagnetic	10.3	17.4, 5.2	−11		12g, 12i
Ho_3Ge_4	antiferromagnetic	11.0	11.4, 6.6	−6.4		12d
Ho_3Ge_4	**antiferromagnetic**	**10.4**	**11.6, 6.2**	**−1**	**57**	**this work**
Er_3Ge_4	antiferromagnetic	9.6	6.9, 3.5			12h, 12i
Er_3Ge_4	**antiferromagnetic**	**9.42**	**6.2, 3.4**	**−3**	**54**	**this work**
Tm_3Ge_4	antiferromagnetic	7.63	2.2, 2.9	−3.8		12e
Tm_3Ge_4	**antiferromagnetic**	**7.55**	**<5**	**−12**		**this work**
Lu_3Ge_4	Pauli paramagnetic					12e

[a] Entries in bold represent data from this work. Previous studies are listed for comparison and referenced accordingly. [b] The effective moments for free ions according to $g_J\sqrt{J(J+1)}$ are Gd^{3+}, 7.94 μ_B; Tb^{3+}, 9.72 μ_B; Dy^{3+}, 10.65; Ho^{3+}, 10.61 μ_B; Er^{3+}, 9.58 μ_B; Tm^{3+}, 7.56 μ_B: see ref 34. [c] Multiple ordering temperatures are typically obtained from calorimetry data.

Temperature dependence of the resistivity (ρ) and the heat capacity (C_p) were taken on single crystals of Ho_3Ge_4 and Er_3Ge_4 (only these were large enough to warrant reproducible measurements) along the direction of the *a*-axis, which was presumed to be the direction of the fastest growth of the needle-shaped crystal (see Experimental Section). The plots are shown in Figure 6; clearly both compounds are metallic with $\rho_{298} \approx 55\ \mu\Omega$ cm. No difference between the measurements upon heating and cooling was observed, which suggests that the charge-carrier concentration and the scat-

(31) Shannon, R. D.; Prewitt, C. T. *Acta Crystallogr.* **1969**, B25, *925*
(32) Another study on the crystal structure of Y_3Ge_4 noted the elongated thermal parameter and proposed a Ge deficiency on the Ge1 site (ref 12b and c). This conclusion is not corroborated by the results from our work on the crystallography of Y_3Ge_4 and the whole family of RE_3Ge_4 (RE = Gd−Tm).
(33) Xia, S.-Q.; Bobev, S. *J. Solid State Chem.* **2006**, *179*, 3371.
(34) (a) Smart, J. S. *Effective Theories of Magnetism*; Saunders: Philadelphia, PA, 1966. (b) Kittel, C. *Introduction to Solid State Physics*, 7th ed.; John Wiley and Sons: Hoboken, NJ, 1996.

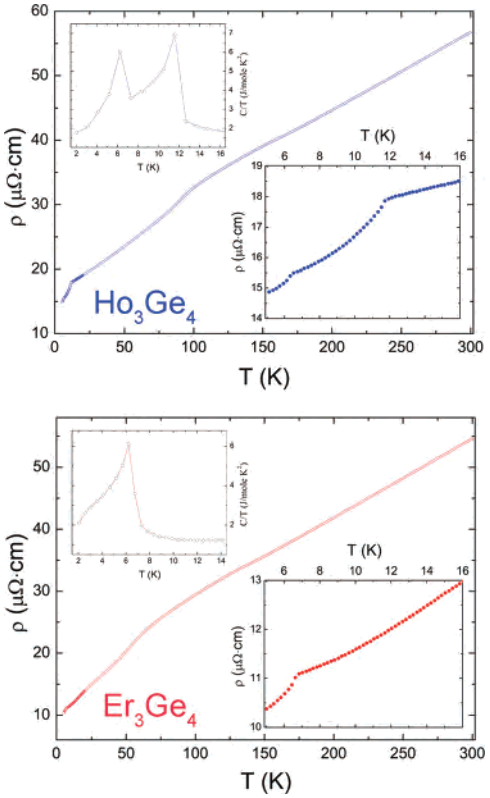

Figure 6. Resistivity (ρ) as a function of the temperature, measured on single crystals of Ho_3Ge_4 and Er_3Ge_4. Lower insets show magnified views at low temperatures; insets in the upper right corners show calorimetry data at low temperature, which are plotted in the format C_p/T vs T.

tering mechanism are independent of the direction of the temperature gradient. Above ~100 K, the dependence of the resistivity with the temperature is virtually linear, as known for the good metals.[34] However, an unexpected change of the slope is seen at around 100 K for Ho_3Ge_4 and around 70 K for Er_3Ge_4. The reason for such a steeper and almost linear decrease at lower temperature is still unknown; possible phase transitions, however, can be ruled out because both $\chi(T)$ and $C_p(T)$ do not provide any evidence to suggest this. At around 12 K for Ho_3Ge_4 and around 6 K for Er_3Ge_4, respectively, there is a sharp drop in $\rho(T)$ (Figure 6, lower insets). These anomalies are most certainly associated with the onset of the first antiferromagnetic order, and the temperature where it occurs coincides with the Néel temperature found by measurements of the magnetic susceptibility (Table 4). As expected, in the antiferromagnetic state, the electrical resistivity exhibits a nearly T^2 temperature dependence according to $\rho(T) = \rho_0 + AT^2$.[34] The heat capacity measurements of Ho_3Ge_4 and Er_3Ge_4 (flux-grown single crystals) show well-defined peaks around the same temperatures (Figure 6, upper insets), confirming the Néel temperatures from the magnetization measurements. The specific heat data also provide evidence for consecutive ordering transitions in both cases, the nature of which has been studied by neutron diffraction and discussed elsewhere.[12d−h]

Conclusions

The new binary compound Gd_3Ge_4 has been synthesized and structurally characterized by single-crystal X-ray diffraction. It crystallizes with the orthorhombic space group *Cmcm* and is, at least formally, an addition to the RE_3Ge_4 family (RE = Y, Tb−Tm).[12] The structure type was re-examined and was found to be better described with a small positional disorder associated with one of the germanium atoms, Ge1. This invokes an alternative rationalization of the structure: instead of square planar Ge, as in the original structural description, the revised model calls for zigzag fragments of two-bonded Ge. The structures of remaining members of the family have also been re-assessed through single-crystal X-ray diffraction studies. These results show that this positional disorder is an intrinsic feature of all and that it becomes progressively smaller as one moves left to right across the lanthanide series. In addition, dc magnetization studies on Gd_3Ge_4 show that the compound orders antiferromagnetically below ~29 K. Electrical resistivity measurements on single-crystals of Ho_3Ge_4 and Er_3Ge_4 confirm that they exhibit typical metallic behavior, in accordance with the electron count.

Acknowledgment. S.B. acknowledges financial support from the University of Delaware. P.H.T. thanks the International Centre for Diffraction Data (ICDD) for the 2007 Ludo Frevel Crystallographic Fellowship. Work at LANL is done under the auspices of U.S. DOE. The authors thank the anonymous reviewer who suggested the Hamilton *R*-value test and Jonathan Hullmann (UD) for proof-reading the manuscript.

Supporting Information Available: A combined X-ray crystallographic file in CIF format, along with details of the synthesis, powder diffraction patterns, plots of fragments of the crystal structures with anisotropic displacement parameters and the corresponding difference Fourier map, coordination polyhedra around the lanthanide atoms, magnetic susceptibility of RE_3Ge_4 (RE = Y, Tb−Tm), and detailed analysis on the structure models with tables with distances. This material is available free of charge via the Internet at http://pubs.acs.org.

IC7009034